Subduction Zone Structure along Sumatra from Receiver Functions[1]

K. Lipke, F. Krüger, D. Rößler, University of Potsdam;   contact: Katrin.Lipke@uni-potsdam.de

Summary

Receiver functions are a good tool to investigate the seismotectonic structure beneath the a seismic station[2]. In this study we apply the method to stations situated on or near Sumatra to find constraints on a more detailed velocity model which should improve earthquake localisation. We estimate shallow Moho-depths (~ 21 km) close to the trench and depths of ~30 km at greater distances. First evidences for the dip direction of the slab of ~60° are provided.
Receiver functions were calculated for 20 stations for altogether 110 earthquakes in the distance range between 30° and 95° from the receiver[3]. However the number of receiver functions per station is strongly variable as it depends on the installation date, the signal-to-noise-ratio of the station and the reliability of the acquisition.

1

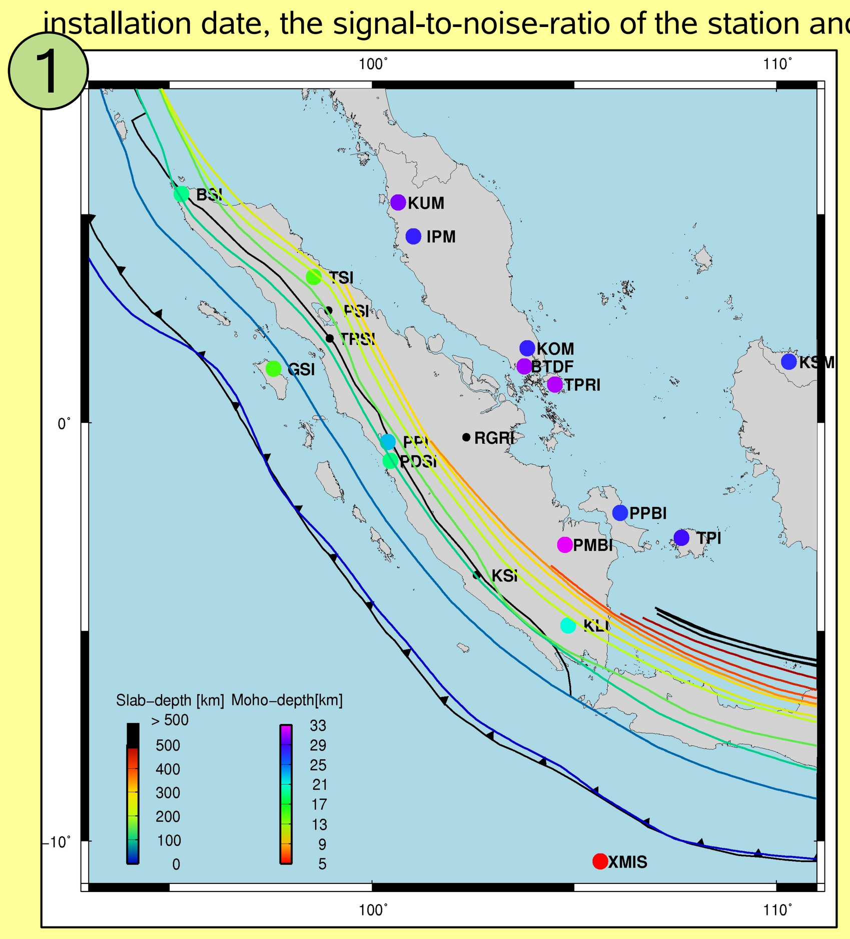

Fig. 1: Map of stations used in this study. If an estimation of the Moho was possible, circles are colored according to depth. Contour lines show the slab depth in steps of 50 km given by the RUM-model[4].

Fig. 2: Epicentres of earthquakes used. Red contour lines give the distance to central Sumatra in [°].

2

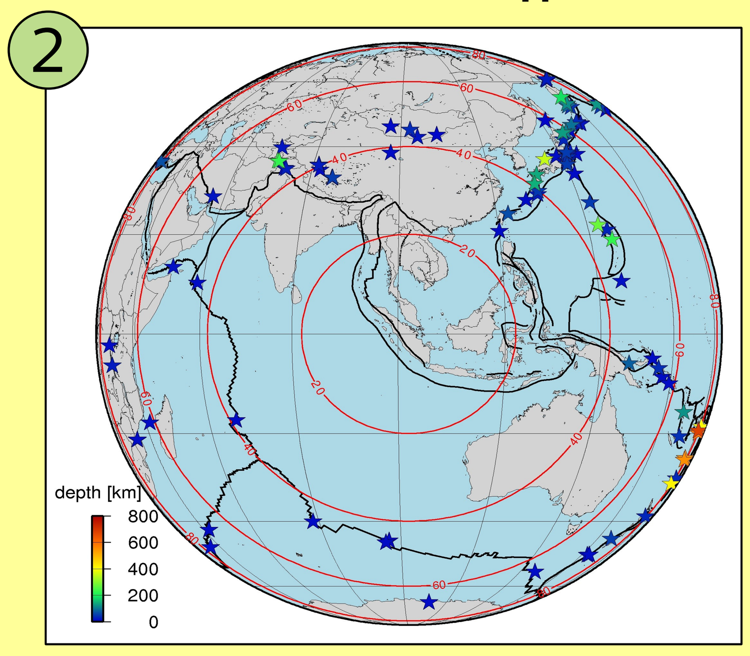

Slab conversions: Theory ...

6

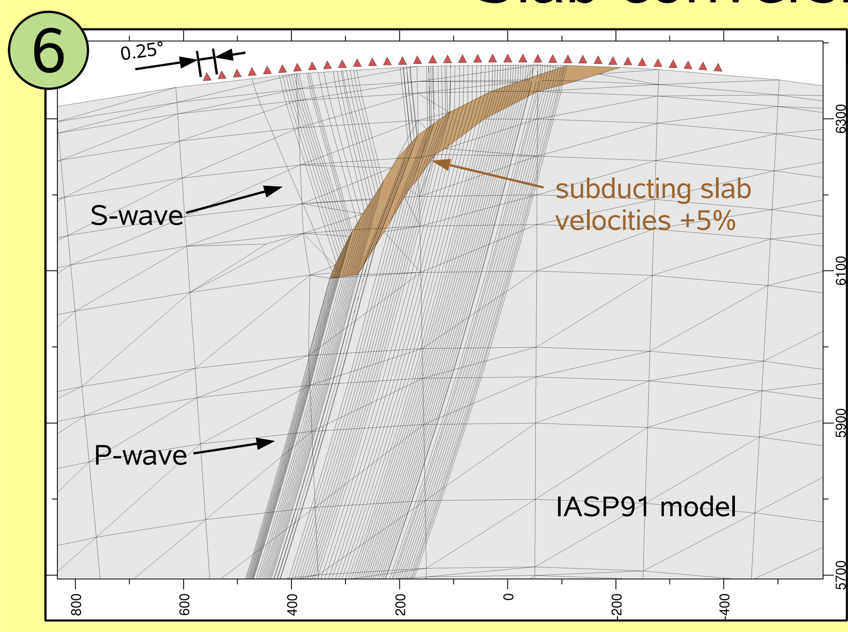

7

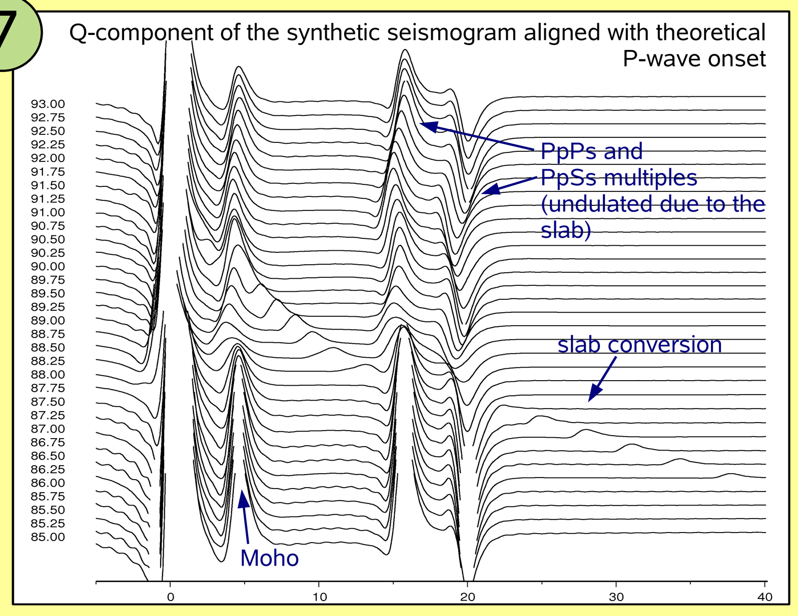

Synthetic seismograms calculated with the help of the Gaussian beam method[7] showing the influence of slab. As the subducting oceanic plate has faster Vp and Vs velocities than the overlying continental lithosphere, a positive signal should be visible in receiver functions.

Fig. 6: Raypaths of P-waves traversing the slab as a and being converted to an S-wave at the top of the subducting lithosphere.
The rightmost station is placed at 85° distance from the epicentre.

Fig. 7: Synthetic seismograms resulting from the model above. The slab-conversion has small amplitude compared to the Moho-conversion and its multiples.
The presence of the slab leads to significant reduction of the amplitudes of all other phases as the rays are refracted and spread over a larger area. In other cases (when the slab was dipping steeper or the velocity contrast was higher) we even observed the extinction of all phases for a certain distance range as the rays were impinging with the critical angle on the lower interface between continental lithosphere and slab.
Due to the small relative amplitudes, detecting the slab conversions may be difficult. The detection is simplified, if the velocity contrast between slab and lithosphere increases.

Moho depth and Vp/Vs-ratio

Fig. 3: Stacked receiver functions plotted according to their distance from the trench. The single traces were corrected for move-out and summed. Finally a lowpass filter at 1s was applied.
We picked the peak probably corresponding to the Moho-conversion with the red bar. The Moho-depth and the delay times of the multiples are calculated with the help of the mean crustal velocities given by Crust2.0[5]. The green bar refers to the PpPs-multiple, the blue bar to the PpSs-multiple. In some cases (e.g. KUM, TPI) we find suitable multiple phases in the stacked traces. In other cases (e.g. PPBI) the velocities should be varied to get a better correlation.
It is striking that the Moho-peak is easier to pick for stations at greater distance from the trench (upper 9 traces) while stations close to the trench show a complicated structure and no multiples can be identified.
(in brackets): number of stacked traces

3

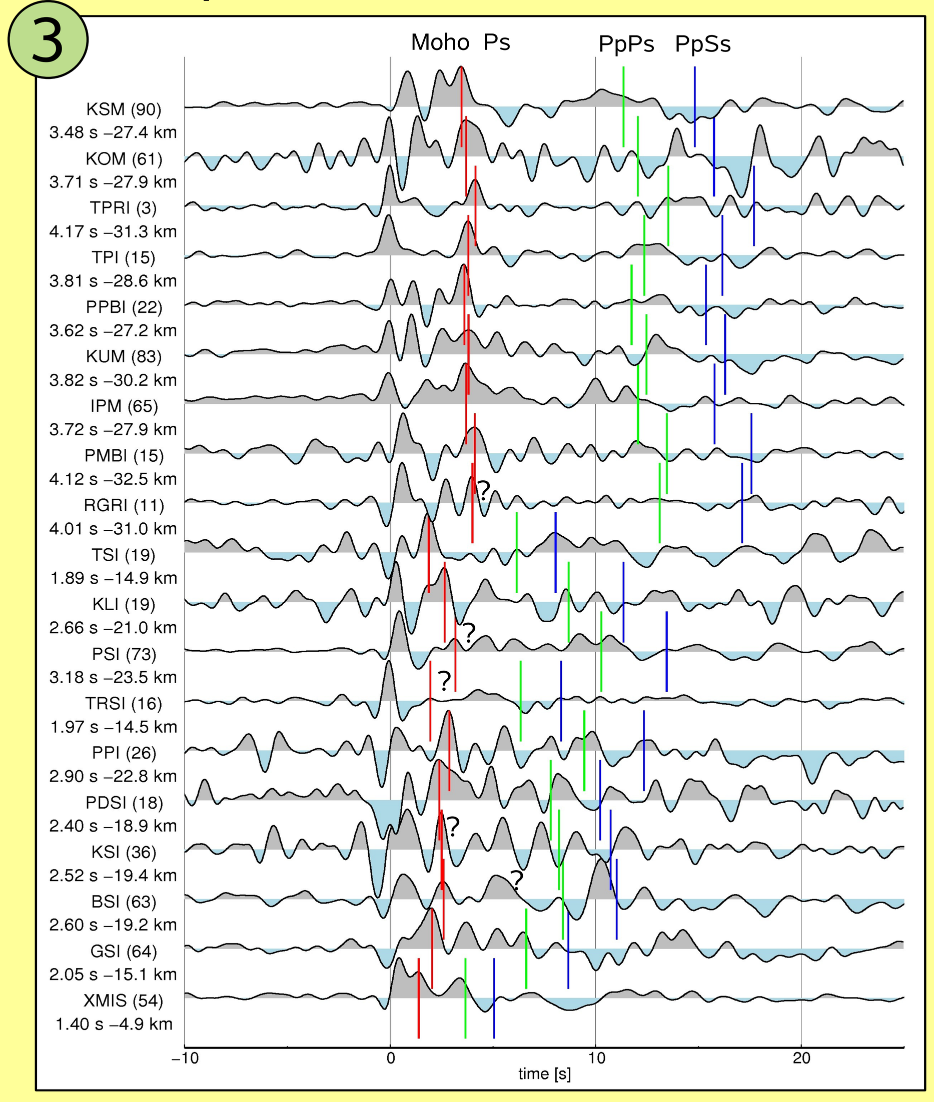

Fig. 4: Result of a grid search over Vp/Vs-ratio κ and depth H. Again best results are found far away from the trench. (The distance of the station to the trench is given in the header.)
Zhu and Kanamori (2000)[6] showed that delay times of conversions and their multiples are strongly dependent on the depth H of the discontinuity and the Vp/Vs-ratio κ in the medium above the discontinuity. Their algorithm results in the grid-search.

4

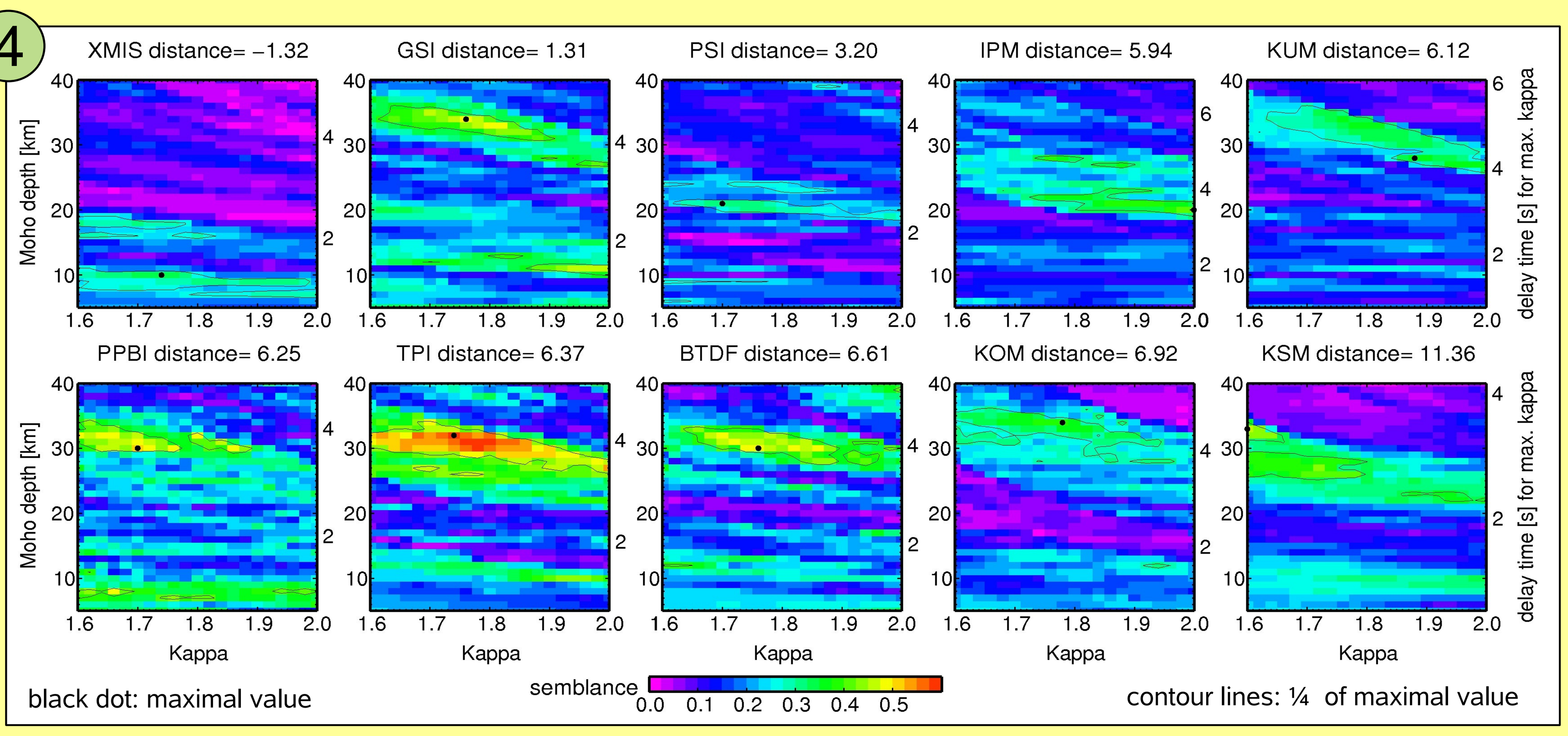

Mantle discontinuities

5

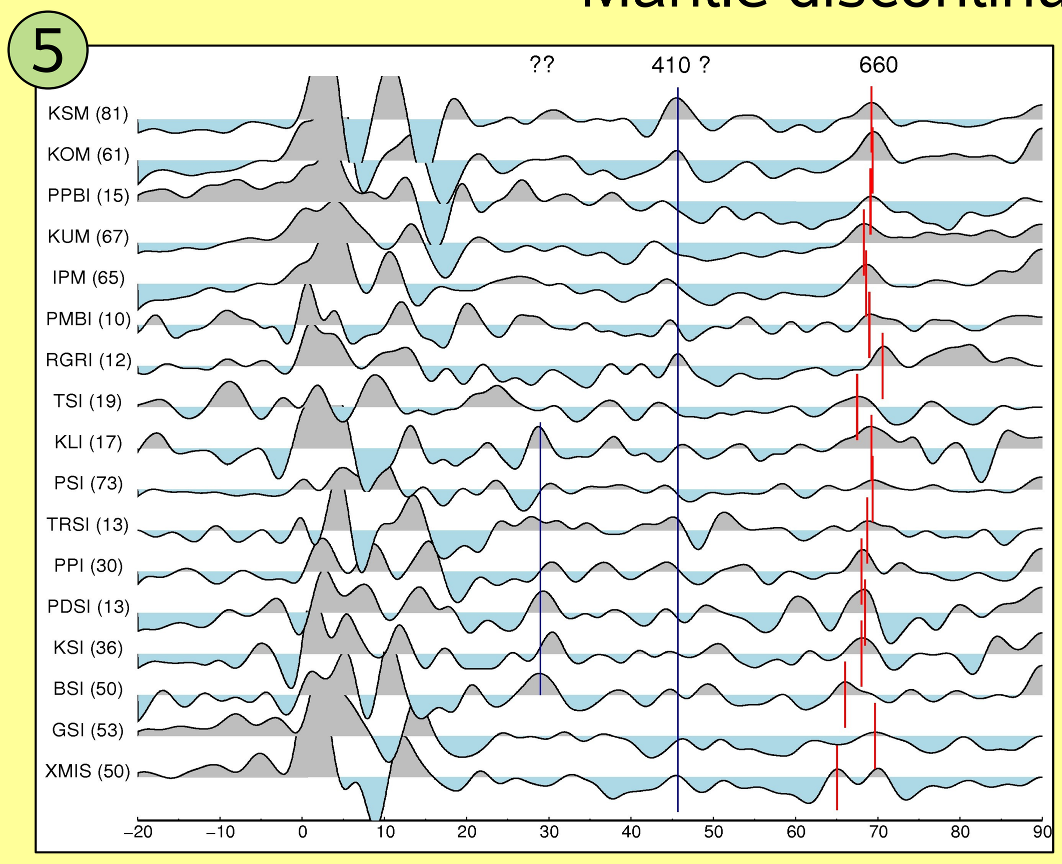

Fig. 5: Move-out corrected and stacked traces filtered with a lowpass filter at 5 s. The 660-km mantle discontinuity can be identified for most stations at delay times between 68 s (KSI) and 70.8 s (RGRI). Station BSI shows a much lower delay time of 66 s. Finally for XMIS no clear decision can be made.
In contrast to the 660-km discontinuity it is difficult to detect the 410-km discontinuity. KSM and KOM show a rather clear signal at 45.7 s. At the other stations no clear peak can be identified.
The theoretical delay times of the 410 and 660-km discontinuities in a IASP91 model are 44.1 and 68.1 s respectively.
Moreover some stations show a signal at 29-30 s. This corresponds to a discontinuity depth of approximately 280 km.

... and reality

8

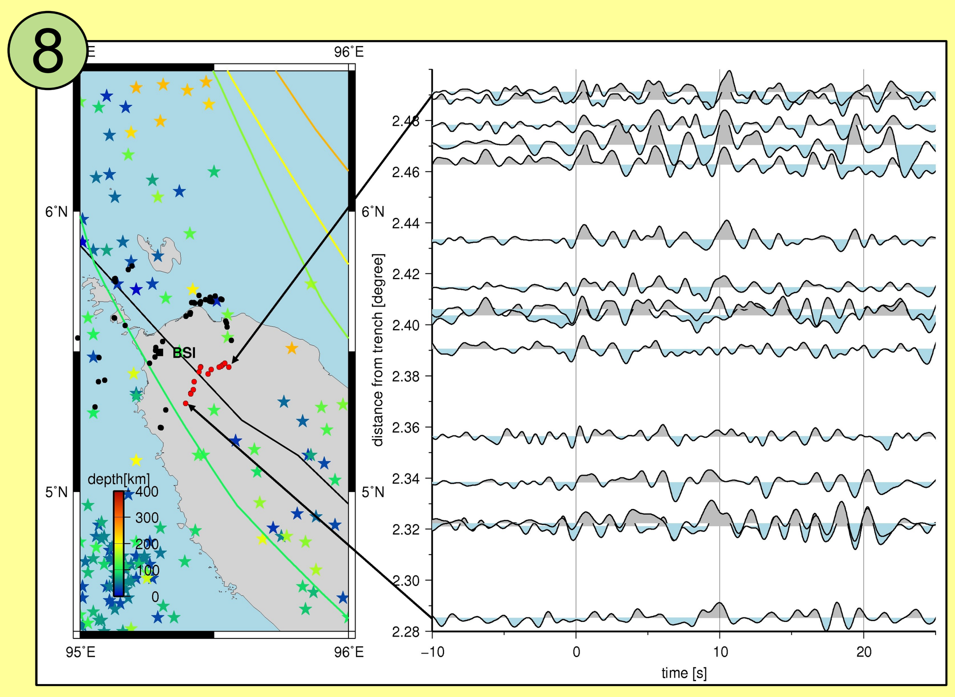

The slab may be revealed from receiver functions at specific azimuth and distances.

Fig. 8: Receiver functions of the red piercing points. Most of them show a peak at ~10 s. The peak occurs at 9.3 s at 2.32° distance from the trench and delays with increasing trench distance to 10.4s at the maximal distance.
For a crustal thickness of 30 km with a crustal P-velocity of 6 km/s and a mantle velocity of 8.1 km/s peaks at 9.3 and 10.4 s correspond to conversions at 87 and 98 km depth, respectively, slightly shallower than the depth of the slab suggested by the RUM model.
Map: station BSI; contour lines: RUM-model; stars: hypocentres from IRIS; dots are the piercing points of the calculated receiver functions at a depth of 100 km.

Fig. 9: Stacked receiver functions of station BSI binned within azimuth of 15°. The probable slab-conversion is picked with the red bars. The same pick times are shown to the left on the T-receiver functions. On the traces at the bottom there is a positive phase on the T-component. At approximately 60° the sign of this phase changes. For a dipping layer a change of sign on T occurs in the direction of the dip. Moreover the largest delay-times are observed for angle between 60° and 90°. This probable dip direction correlates well with the 330° strike direction of the trench close to the station.

9

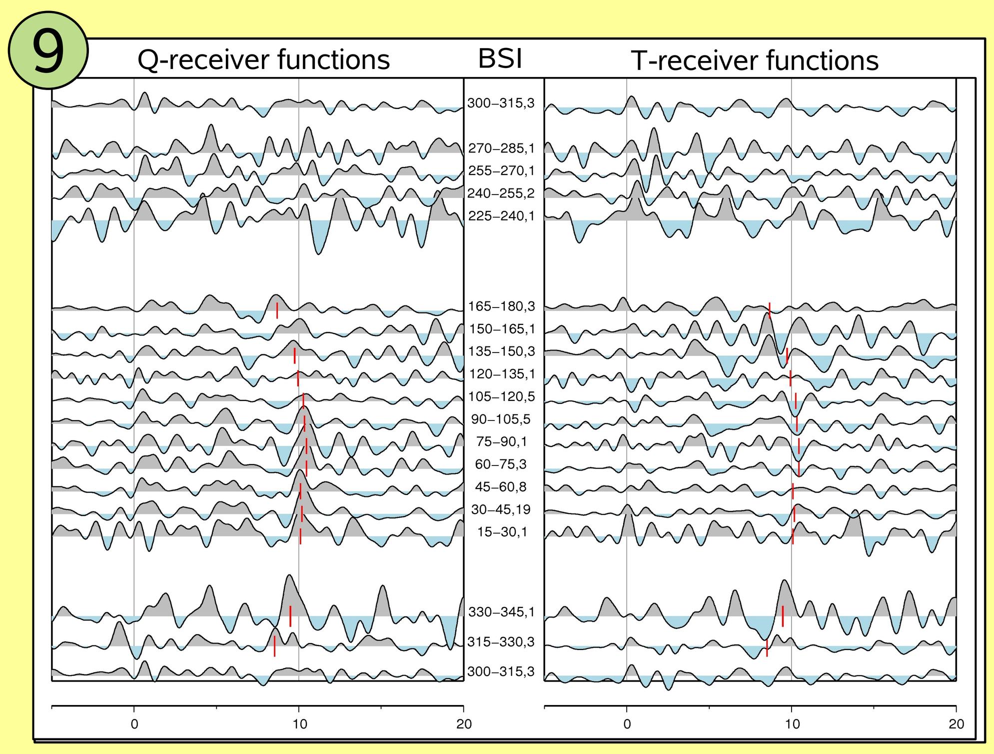

Dipping layers

10

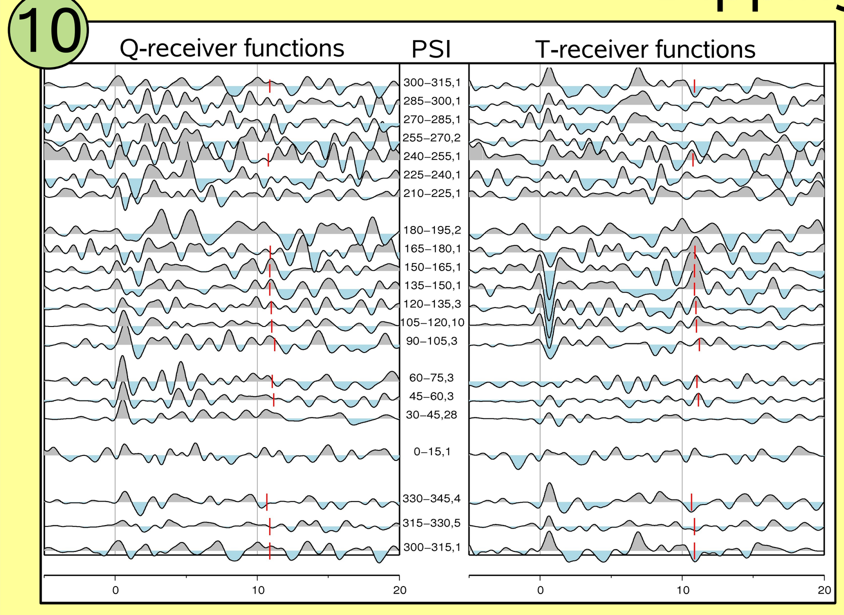

11

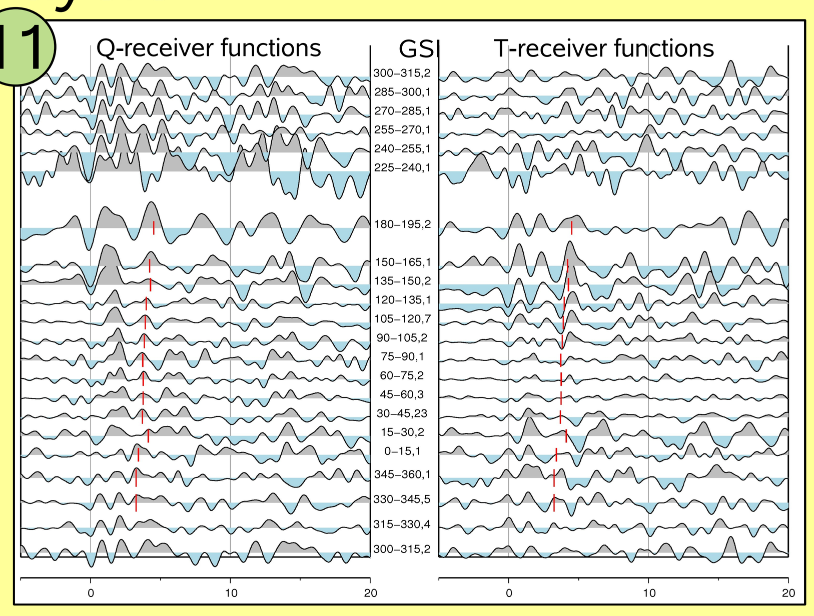

Fig. 10: Azimuthal stacked receiver functions for station PSI. On the T-component we observe again a 180° symmetry for a peak at ca. 11 s (red bars picked on T). The change of sign occurs between 0° and 45°. The identification of the appropriate peak on Q is difficult. Another coherent signal is observed for small delay times.

Fig. 11: Azimuthal stacked receiver functions for station GSI (red bars picked on Q). The change of sign for the signal at 3-4 s indicates a dipping interface in the direction of 60°. The corresponding depth of ca. 40 km correlates well with the RUM-model.

12

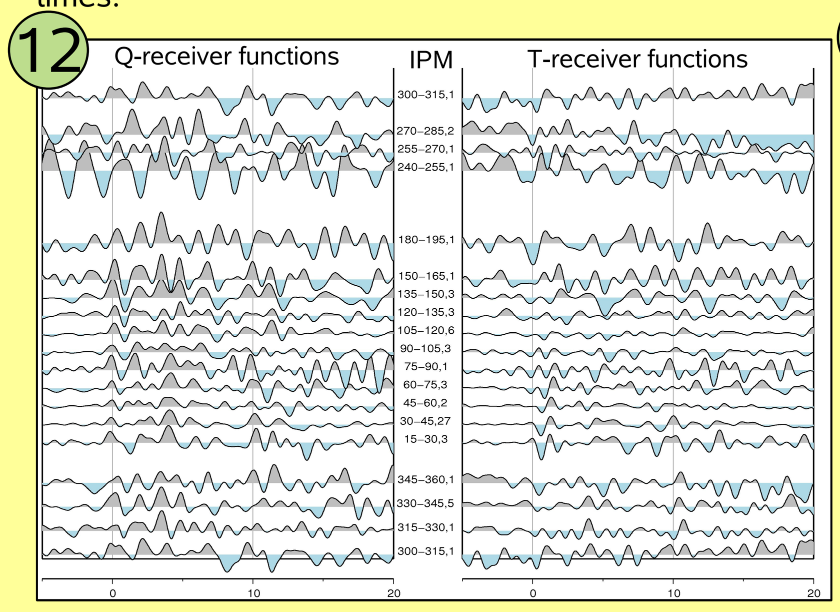

13

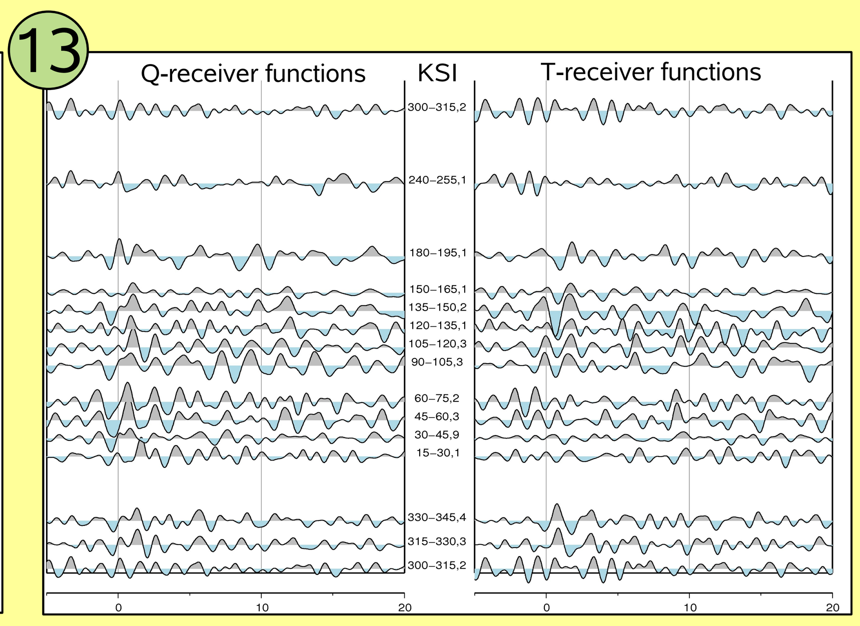

Fig. 12 and 13: Azimuthal stacked receiver functions for station IPM and KSI respectively. Coherent signals may be identified, especially for small delay times which correspond to crustal structures.

(1) This study is done in the context of a diploma thesis.
(2) Yuan, X. et al, Lithospheric and upper mantle structure of southern Tibet from a seismological passive source experiment, *J. Geophys. Res.*, 102(B12), 27491-27500, December 1997.
(3) Data were provided by GEFON, IRIS and ISC
(4) Gudmundsson, Ó., and M. Sambridge (1998), A regionalized upper mantle (RUM) seismic model, *J. Geophys. Res.*,103(B4), 7121–7136.
(5) http://mahi.ucsd.edu/Gabi/rem.html
(6) L. Zhu and H. Kanamori. Moho depth variation in southern california from teleseismic receiver functions. *Journal of Geophysical Research*, 105 2969–2980, February 2000.
(7) Weber,M, Computation of body wave seismograms in absorbing 2D-media using the Gaussian beam method: comparison with exact methods, *Geophysical Journal*, 92, 9-24, January 1988